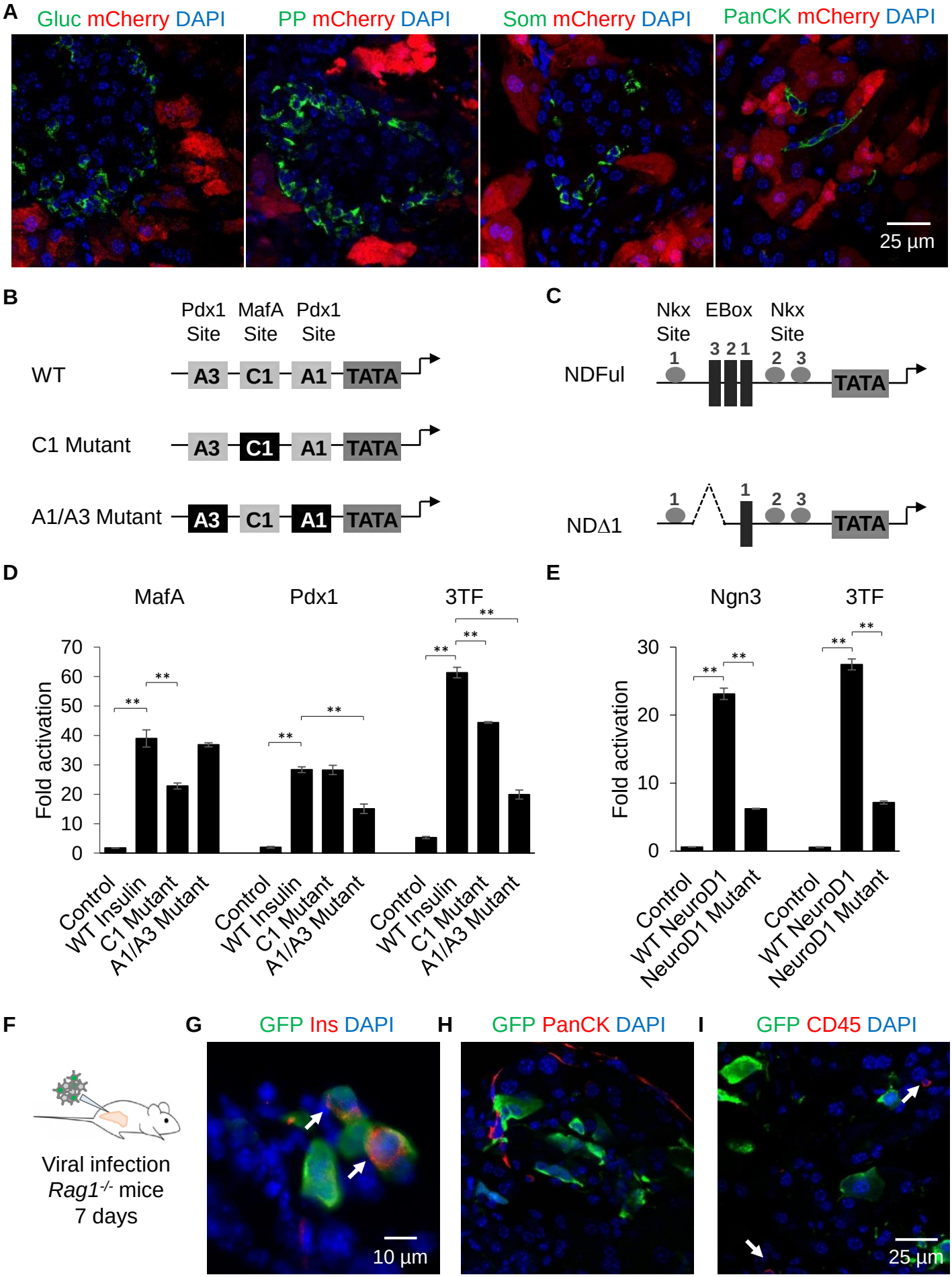
A
Gluc mCherry DAPI
PP mCherry DAPI
Som mCherry DAPI
PanCK mCherry DAPI
25 µm
B
Pdx1 Site
MafA Site
Pdx1 Site
WT
C1 Mutant
A1/A3 Mutant
A3
C1
A1
TATA
C
Nkx Site
EBox
Nkx Site
NDFul
NDΔ1
1
2
3
TATA
D
MafA
Pdx1
3TF
Fold activation
Control
WT Insulin
C1 Mutant
A1/A3 Mutant
E
Ngn3
3TF
Fold activation
Control
WT NeuroD1
NeuroD1 Mutant
F
Viral infection
Rag1-/- mice
7 days
G
GFP Ins DAPI
10 µm
H
GFP PanCK DAPI
I
GFP CD45 DAPI
25 µm

Figure S1. Validation of the mouse model, Related to Figure 1. (A) After 1 day of dox, mCherry was not expressed in glucagon-, pancreatic polypeptide-, or somatostatin-expressing endocrine cells, or in ductal cells, marked by PanCK staining. (B) Promoter constructs used for Dual Luciferase Assay to test the functionality of the 2A peptide modified MAFA and PDX1 proteins. Constructs used were a wild-type (WT), MafA-binding mutant (mutant C1), or Pdx1-binding mutant (double mutant A1/A3) of the insulin promoter fused to luciferase. (C) Promoter constructs used for Dual Luciferase Assay to test the functionality of the 2A peptide modified NEUROG3 protein. Constructs used were a WT *NeuroD1* promoter fused to luciferase (NDFul) or a *NeuroD1* promoter containing a deletion of the Neurog3 binding site fused to luciferase (NDΔ1). (D) Dual Luciferase Assay was performed in transfected HeLa cells using either the WT or mutated insulin promoter constructs. Control was no transcription factors. Data are represented as mean ± SEM. **p < 0.001, student's t-test, n=3. (E) Dual Luciferase Assay was performed in transfected Panc1 cells using either the WT or mutated *NeuroD1* promoter fused to luciferase. Control was no transcription factors. Data are represented as mean ± SEM. **p < 0.001, student's t-test, n=3. (F) The splenic lobe of the dorsal pancreas of 8 week old *Rag1*$^{-/-}$ mice was injected with 100 µl of a purified 3TF-expressing adenovirus (AdV-CMV-3TF; $2x10^{10}$ pfu) and a GFP-expressing adenovirus (AdV-CMV-GFP, $1x10^{9}$ pfu). Animals were euthanized 7 days later. (G) Pancreatic immunofluorescence staining of insulin and GFP. Arrows indicate infected acinar cells that have been reprogrammed into insulin-expressing cells. (H) Representative pancreatic immunofluorescence staining of PanCK (I) and CD45, 7 days post AdV-CMV-3TF, infection indicates that adenoviral delivery of our 3TF construct did not result in a potent inflammatory response or ADM.

A

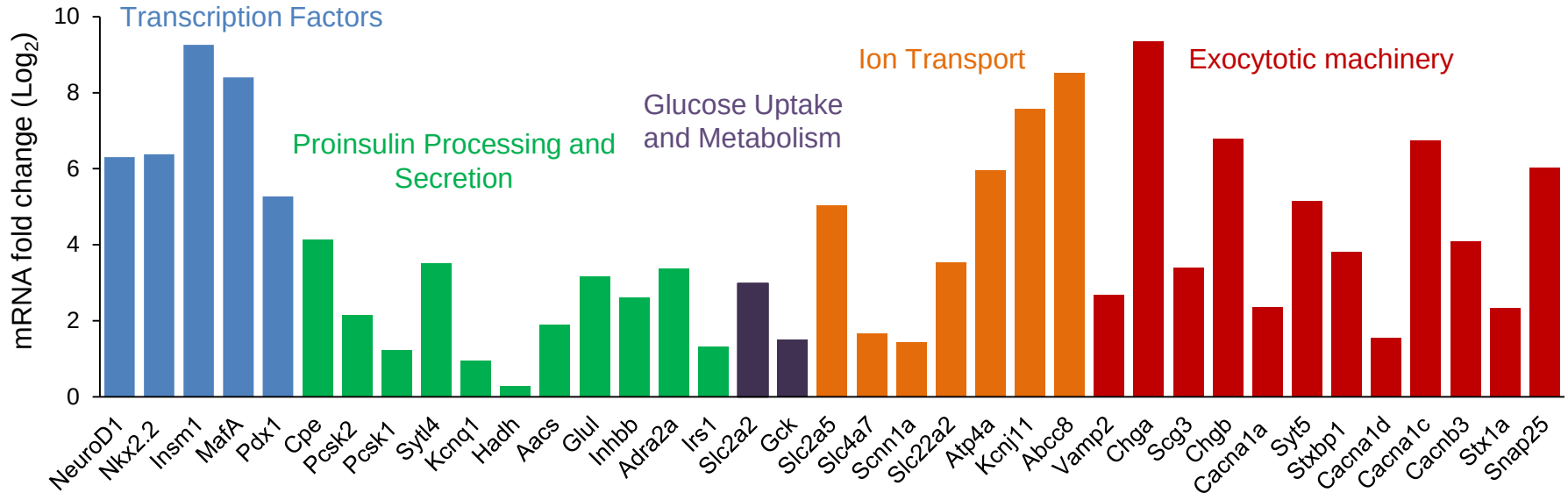
Transcription Factors
Proinsulin Processing and Secretion
Glucose Uptake and Metabolism
Ion Transport
Exocytotic machinery
mRNA fold change (Log2)
0
2
4
6
8
10
NeuroD1
Nkx2.2
Insm1
MafA
Pdx1
Cpe
Pcsk2
Pcsk1
Sytl4
Kcnq1
Hadh
Aacs
Glul
Inhbb
Adra2a
Irs1
Slc2a2
Gck
Slc2a5
Slc4a7
Scnn1a
Slc22a2
Atp4a
Kcnj11
Abcc8
Vamp2
Chga
Scg3
Chgb
Cacna1a
Syt5
Stxbp1
Cacna1d
Cacna1c
Cacnb3
Stx1a
Snap25

B

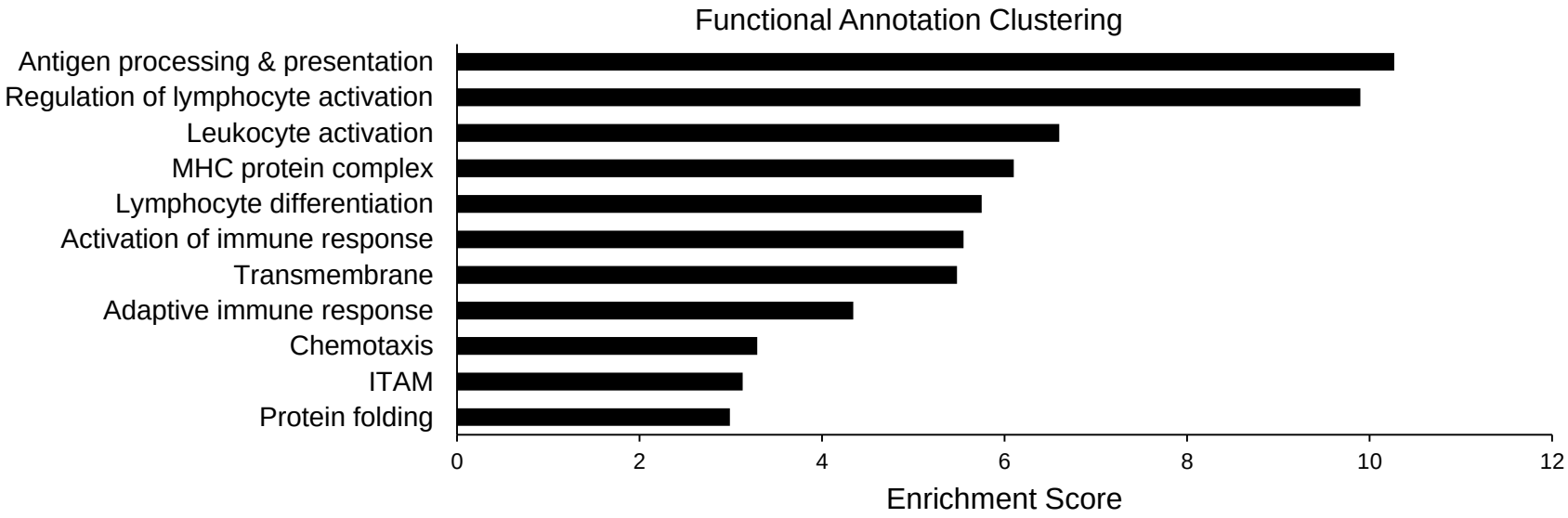
Functional Annotation Clustering
Antigen processing & presentation
Regulation of lymphocyte activation
Leukocyte activation
MHC protein complex
Lymphocyte differentiation
Activation of immune response
Transmembrane
Adaptive immune response
Chemotaxis
ITAM
Protein folding
0
2
4
6
8
10
12
Enrichment Score

Figure S2. Reprogrammed cells do not resemble endogenous β-cells, Related to Figure 2. (A) Fold changes (log2 scale; pseudocounts added) in the expression of β-cell specific genes calculated from our RNA-seq data set of 7 day 3TF-induced acinar cells compared to uninduced acinar cells. These mRNAs were identified as significantly differentially expressed by both edgeR and PADE. (B) The top eleven functional annotation clusters compiled from the top 200 up-regulated genes in our RNA-seq data set of 7 day 3TF-induced acinar cells compared to uninduced acinar cells using DAVID analysis.

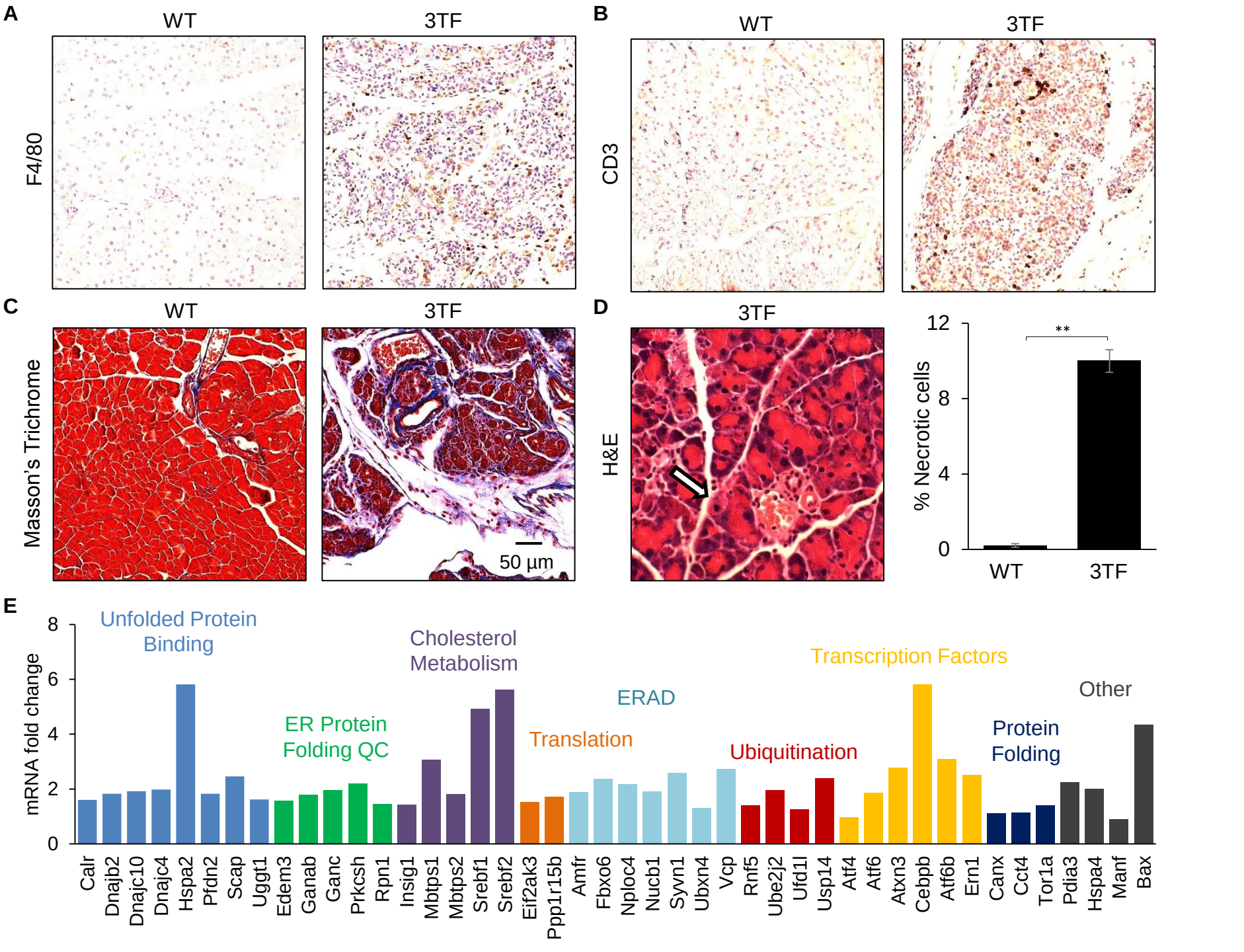
A
WT
3TF
F4/80
B
WT
3TF
CD3
C
WT
3TF
Masson's Trichrome
50 µm
D
3TF
H&E
12
8
4
0
% Necrotic cells
**
WT
3TF
E
mRNA fold change
8
6
4
2
0
Unfolded Protein Binding
Cholesterol Metabolism
ER Protein Folding QC
ERAD
Translation
Transcription Factors
Ubiquitination
Protein Folding
Other
Calr
Dnajb2
Dnajc10
Dnajc4
Hspa2
Pfdn2
Scap
Uggt1
Edem3
Ganab
Ganc
Prkcsh
Rpn1
Insig1
Mbtps1
Mbtps2
Srebf1
Srebf2
Eif2ak3
Ppp1r15b
Amfr
Fbxo6
Nploc4
Nucb1
Syvn1
Ubxn4
Vcp
Rnf5
Ube2j2
Ufd1l
Usp14
Atf4
Atf6
Atxn3
Cebpb
Atf6b
Ern1
Canx
Cct4
Tor1a
Pdia3
Hspa4
Manf
Bax

Figure S3. Transgene-mediated 3TF-overexpression causes a potent inflammatory response, Related to Figure 3. (A) Representative F4/80, (B) CD3, and (C) Masson's trichrome stain of WT and *Ptf1a*$^{rtTA/+}$; *Rosa26*$^{3TF.mCherry/+}$ (3TF) mice at 7 days dox treatment. (D) Acinar cell necrosis (arrow) was observed in the pancreata of 3TF mice treated with dox for 2 days. (E) Necrosis was measured on tissue sections stained with H&E from WT mice and 3TF mice treated with dox for 2 days. Necrosis is represented as the percentage of necrotic acinar cells among acinar cells. Three mice per group and over 1,000 acinar cells were counted for each mouse. Data are represented as mean $\pm$ SEM. **$p < 0.001$, student's t-test. (E) Fold changes (pseudocounts added) in the expression of key genes recognizing and responding to misfolded protein accumulation in the ER calculated from our RNA-seq data set of 7 day 3TF-induced acinar cells compared to uninduced acinar cells. These mRNAs were found to be differentially expressed by both edgeR and PADE.

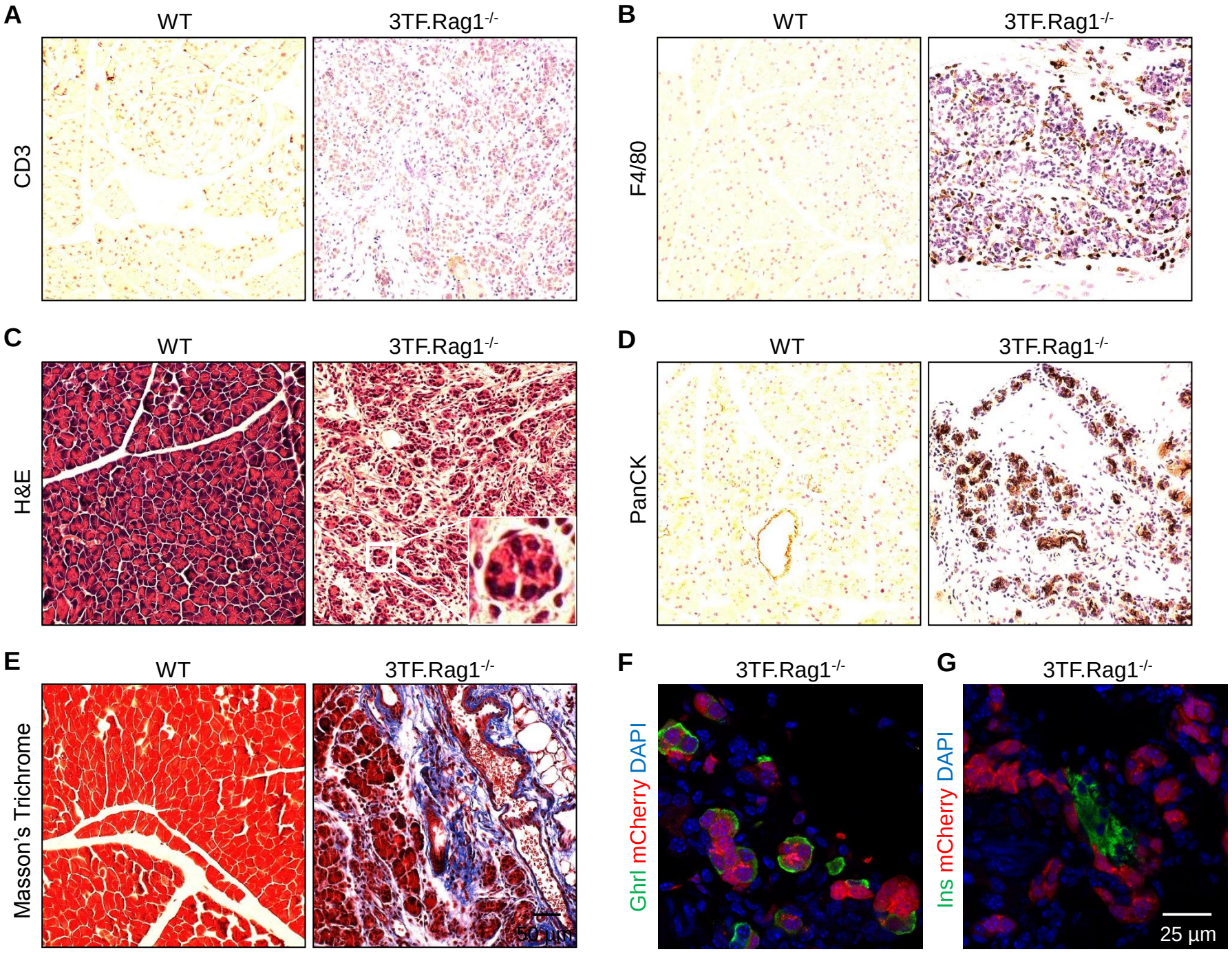
A
WT
3TF.Rag1-/-
CD3
B
WT
3TF.Rag1-/-
F4/80
C
WT
3TF.Rag1-/-
H&E
D
WT
3TF.Rag1-/-
PanCK
E
WT
3TF.Rag1-/-
Masson's Trichrome
50 µm
F
3TF.Rag1-/-
Ghrl mCherry DAPI
G
3TF.Rag1-/-
Ins mCherry DAPI
25 µm

Figure S4. Rag1 deletion does not alter the outcome of 3TF-mediated acinar cell reprogramming, Related to Figure 3. (A) Representative CD3 stain of WT and *Ptf1a*$^{rtTA/+}$*; Rosa26*$^{3TF.mCherry/+}$*; Rag1*$^{-/-}$ (3TF. Rag1$^{-/-}$) mice at 7 days dox (2.0 mg/ml) treatment. No CD3^{+} cells are observed in WT or 3TF.Rag1$^{-/-}$ mice. (B) Representative F4/80 stain of WT and 3TF. Rag1$^{-/-}$ mice at 7 days dox treatment. (C) H&E staining of WT and 3TF. Rag1$^{-/-}$ mice after 7 days dox administration. Pancreas of 3TF. Rag1$^{-/-}$ mice is characterized by the presence of abundant tubular complexes (inset). (D) Representative PanCK stain and (E) Masson's trichrome stain of WT and 3TF. Rag1$^{-/-}$ mice at 7 days dox treatment. (F) Pancreatic immunofluorescence ghrelin staining of 3TF. Rag1$^{-/-}$ mice at 7 days dox treatment. Multiple mCherry^{+} cells co-express ghrelin. (G) Pancreatic immunofluorescence insulin staining of 3TF. Rag1$^{-/-}$ mice at 7 days dox treatment. No mCherry^{+} cells that co-express insulin were observed despite examining over 1,000 mCherry^{+} cells.

A

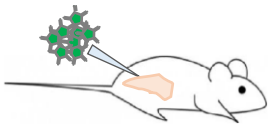

AdV-CMV-GFP infection of 3TF mice
7 days dox

B

GFP mCherry

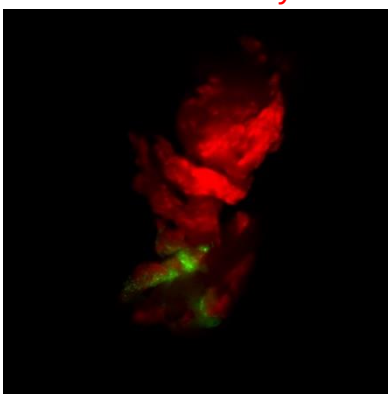

C

GFP mCherry Ghrl DAPI

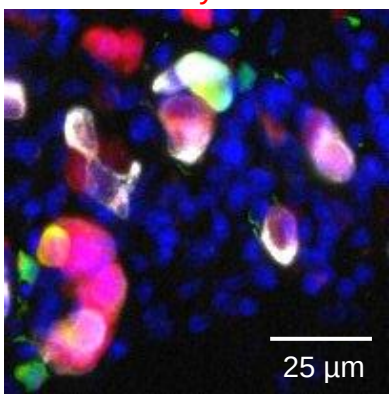

D

GFP mCherry Ins DAPI

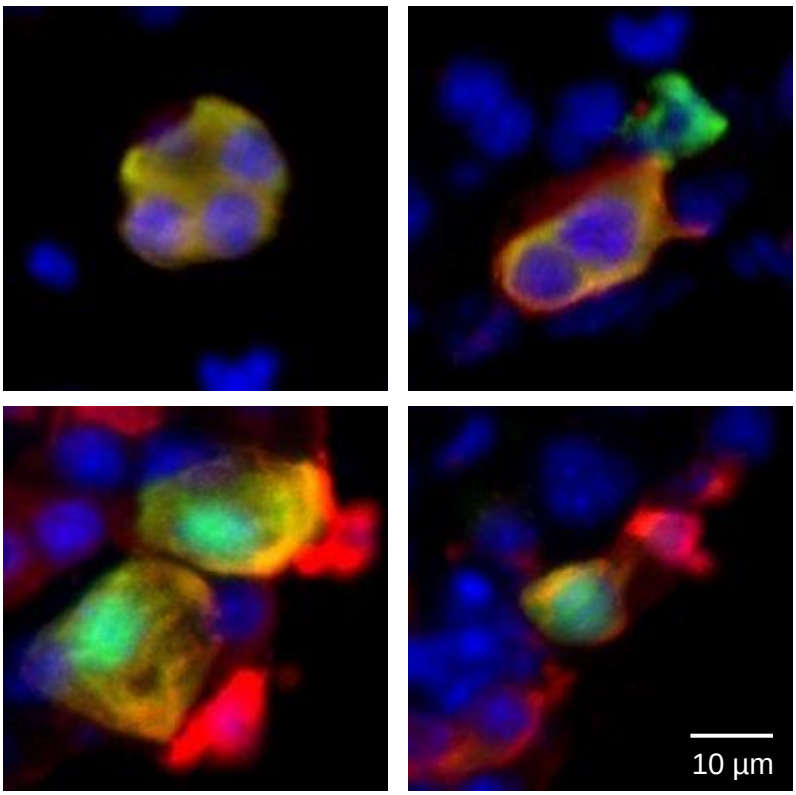

GFP⁺mCherry⁺ cells	**615**
GFP⁺mCherry⁺insulin⁺ cells	**0**

Figure S5. Adenoviral infection is not required for 3TF-mediated A→β reprogramming, Related to Figure 3. (A) Schematic to test if the adenoviral capsid or viral infection is required for 3TF-mediated A→β reprogramming. 6- 8 week old 3TF mice were injected with 100 µl of AdV-CMV-GFP ($1x10^9$ pfu) then administered dox (2.0 mg/ml) for 7 days. (B) Representative pancreas of 3TF mice infected with an AdV-CMV-GFP and administered 2.0 mg/ml of dox at 7 days. Successful pancreatic injection of the AdV-CMV-GFP is demonstrated by GFP fluorescence. (C) Pancreatic immunofluorescence ghrelin staining of 3TF mice at 7 days of dox treatment and AdV-CMV-GFP infection. Multiple $mCherry^+$ cells co-express ghrelin and the GFP-expressing adenovirus. (D) Pancreatic immunofluorescence insulin staining of 3TF mice at 7 days of dox treatment and AdV-CMV-GFP infection. No $mCherry^+$ cells that co-express insulin and GFP were observed despite examining over 600 $mCherry^+/GFP^+$ cells.

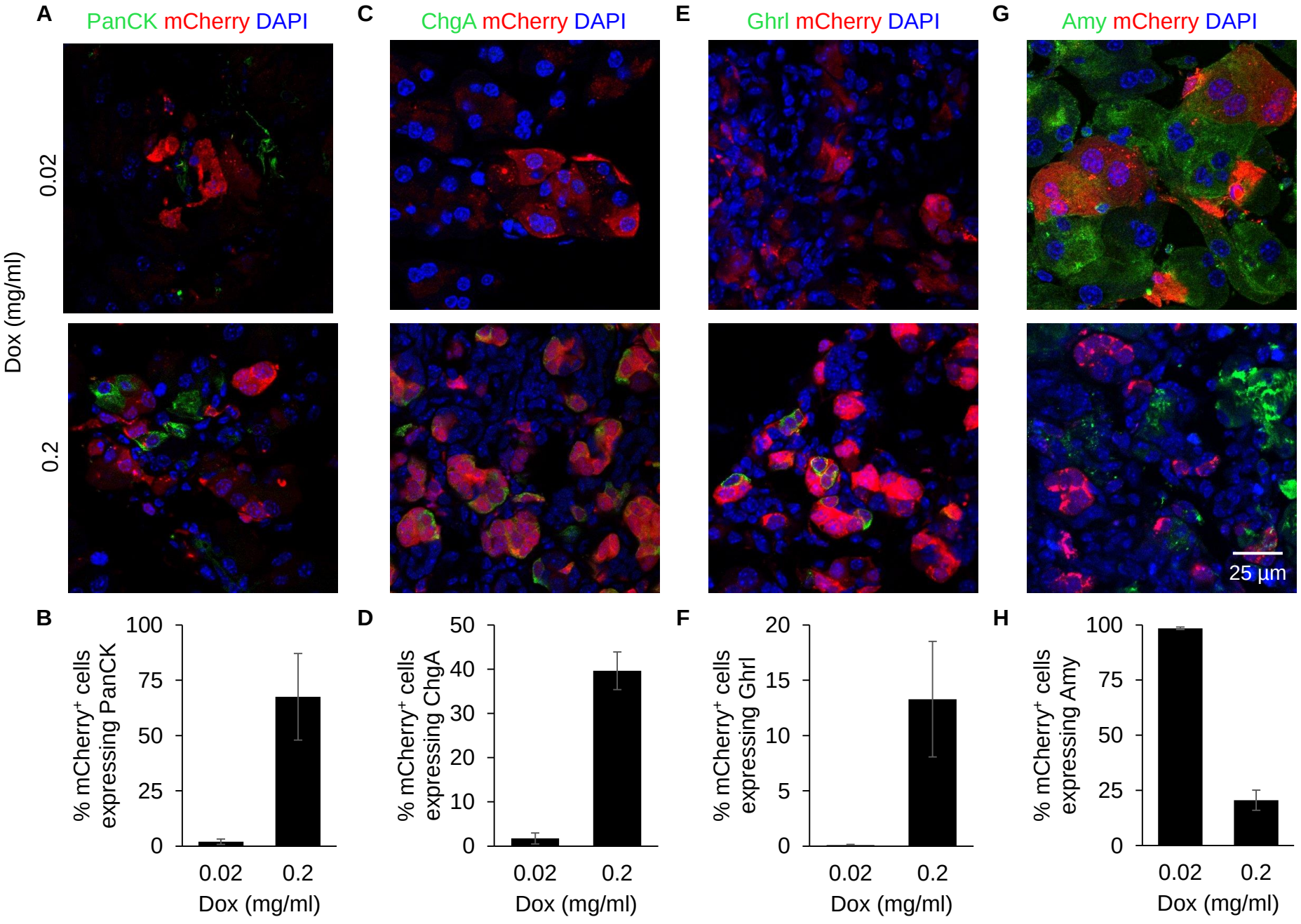
A
PanCK mCherry DAPI
C
ChgA mCherry DAPI
E
Ghrl mCherry DAPI
G
Amy mCherry DAPI
Dox (mg/ml)
0.02
0.2
25 µm
B
% mCherry+ cells expressing PanCK
100
75
50
25
0
0.02
0.2
Dox (mg/ml)
D
% mCherry+ cells expressing ChgA
50
40
30
20
10
0
0.02
0.2
Dox (mg/ml)
F
% mCherry+ cells expressing Ghrl
20
15
10
5
0
0.02
0.2
Dox (mg/ml)
H
% mCherry+ cells expressing Amy
100
75
50
25
0
0.02
0.2
Dox (mg/ml)

Figure S6. The magnitude of 3TF expression affects the outcome of 3TF-mediated acinar cell reprogramming, Related to Figure 4. (A) Immunostaining for PanCK in pancreata of 3TF mice administered varying concentrations of dox for 7 days. (B) Percentage of $PanCK^+$ cells among $mCherry^+$ cells. Three mice per time point and over 500 $mCherry^+$ cells counted for each mouse. Data are represented as mean ± SEM. (C) Immunostaining for chromogranin A in pancreata of 3TF mice administered varying concentrations of dox for 7 days. (D) Percentage of chromogranin A^+ cells among $mCherry^+$ cells. Three mice per time point and over 500 $mCherry^+$ cells counted for each mouse. Data are represented as mean ± SEM. (E) Immunostaining for ghrelin in pancreata of 3TF mice administered varying concentrations of dox for 7 days. (F) Percentage of $ghrelin^+$ cells among $mCherry^+$ cells. Three mice per time point and over 500 $mCherry^+$ cells counted for each mouse. Data are represented as mean ± SEM. (G) Pancreatic immunofluorescence staining of amylase in pancreata of 3TF mice administered varying concentrations of dox for 7 days. (H) Percentage of $amylase^+$ cells among $mCherry^+$ cells. Three mice per time point and over 500 $mCherry^+$ cells counted for each mouse. Data are represented as mean ± SEM.

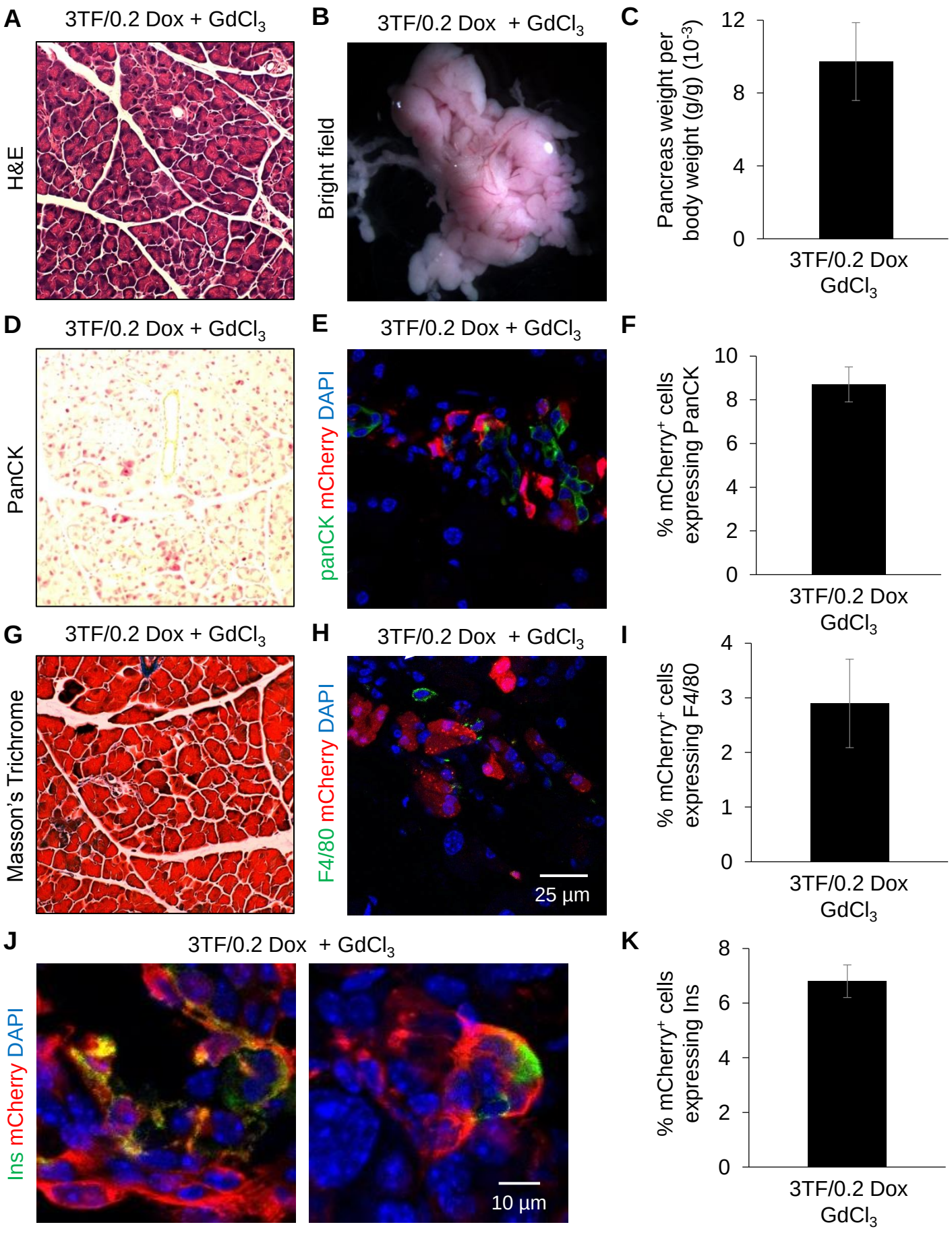
A
3TF/0.2 Dox + GdCl3
H&E
B
3TF/0.2 Dox + GdCl3
Bright field
C
Pancreas weight per body weight (g/g) (10-3)
12
8
4
0
3TF/0.2 Dox
GdCl3
D
3TF/0.2 Dox + GdCl3
PanCK
E
3TF/0.2 Dox + GdCl3
panCK mCherry DAPI
F
% mCherry+ cells expressing PanCK
10
8
6
4
2
0
3TF/0.2 Dox
GdCl3
G
3TF/0.2 Dox + GdCl3
Masson's Trichrome
H
3TF/0.2 Dox + GdCl3
F4/80 mCherry DAPI
25 µm
I
% mCherry+ cells expressing F4/80
4
3
2
1
0
3TF/0.2 Dox
GdCl3
J
3TF/0.2 Dox + GdCl3
Ins mCherry DAPI
10 µm
K
% mCherry+ cells expressing Ins
8
6
4
2
0
3TF/0.2 Dox
GdCl3

Figure S7. Simultaneously lowering the concentration of dox and depleting macrophages reduces inflammation but does not further increase A→β reprogramming, Related to Figure 6. 3TF mice were simultaneously administered a low concentration of dox (0.2 mg/ml) and intravenously injected with the macrophage toxin $GdCl_3$ for 7 days. (A) Representative H&E staining and (B) pancreata from mice reveals that this dual treatment preserves pancreas histology and mass. (C) Pancreatic weight per body weight. Data are represented as mean ± SEM, n=3. (D) Pancreatic PanCK staining and (E) immunofluorescence staining of PanCK reveals that this dual treatment prevents ADM. (F) Percentage of $PanCK^+$ cells among $mCherry^+$ cells at 7 days of dox. Three mice per time point and over 500 $mCherry^+$ cells counted per mouse. Data are represented as mean ± SEM. (G) Representative Masson's trichrome stain and (H) immunofluorescence staining of F4/80 reveals that this dual treatment reduces inflammation. (I) Percentage of $F4/80^+$ cells among $DAPI^+$ cells. Three mice per time point and over 1,000 $DAPI^+$ cells counted. Data are represented as mean ± SEM. (J) After 7 days of dox, a few scattered $insulin^+$ cells that expressed mCherry were observed. (D) Percentage of $insulin^+$ cells among $mCherry^+$ cells. Three mice per time point and over 1,000 $mCherry^+$ cells counted. Data are represented as mean ± SEM.

Supplemental Tables

Table S1. RNA-seq analysis of FACS-purified acinar cells and 1 and 7 day 3TF-induced acinar cells, Related to Figure 2. Values are PORT-normalized counts. Acinar cells are from 60 day old mice

Table S2. Differentially expressed genes after 1 and 7 days of 3TF induction, Related to Figure 2. Determined to be differentially expressed by both edgeR and PADE. Differential Expression (DE) compared to P60 acinar cells

Table S3. Beta-cell specific genes not identified as significantly differentially expressed after 7 days of 3TF induction, Related to Figure 2. Determined to not be differentially expressed by both edgeR and PADE. Differential Expression compared to P60 acinar cells.

Table S4. Increased expression of $Ca2^+$ Channels in 7 day dox-treated mice, Related to Figure 3. Determined to be differentially expressed by both edgeR and PADE. Fold change compared to P60 acinar cells.

Table S5. Estimated number of new Beta-like cells produced, Related to Figure 7

Estimated number of new Beta-like cells	
Cells in Pancreas [1]	57.5×10^6
$mCherry^+$ Cells*	10.9×10^6
New β-like cells**	6.5×10^5
[1] See Ref (Dore et al., 1981)	
*19% of the cells present in the pancreas after 7 days of dox (2 mg/ml) and $GdCl_3$ treatment are $mCherry^+$	
** 6% of the $mCherry^+$ cells express insulin after 7 days of dox (2 mg/ml) and $GdCl_3$ treatment	

Table S6. Primers used, Related to Figure 1 and 6

Primer	**Sequence (5' to 3')**	**PCR product (bps)**	**Application**
Rosa26.S1 Hygro-3'	AGACTTATCTACCTCATAGGTG GTGAGAACAGAGTACCTACAT	761	Screening of RMCE-derived mESCs
Rosa26.R1 Rosa26.S2	GAGGATCATAATCAGCCATACC TCACAAGCAATAATAACCTGTAGT	512	Screening of mESCs and genotyping of *ROSA*$^{3TF.mCherry}$ allele
F-p48 R-5'p48	CCTTCTGACTTCTCCAAGAAGGCA CCCTTTATGCCTGGCATTTCACTG	Targeted: 670 Wild-type: 636	Genotyping *of Ptf1a*^{rtTA} allele
Ins1-Fwd Ins1-Rv	CCAGCCCTTAGTGACCAGCTAT CCCAGGCTTTTGTCAAACAG	143 (exons 1-2)	RT-qPCR of *Ins1*
Ins2-Fwd Ins2-Rv	CCACCCAGGCTTTTGTCAAA CCCAGCTCCAGTTGTTCCAC	149 (exons 2-3)	RT-qPCR of *Ins2*
Hprt-Fwd Hprt-Rv	TACGAGGAGTCCTGTTGATGTTGC GGGACGCAGCAACTGACATTTCTA	138 (exon 9)	RT-qPCR of *Hprt* (Endogenous control)

Supplemental Experimental Procedures

Mutant alleles and genotyping. Both the *Rosa26*$^{3TF.mCherry}$ and *Ptf1a*^{rtTA} alleles were derived by recombinase mediated cassette exchange using mouse ES cells (mESC) that had been previously engineered to contain loxed cassette acceptor alleles with methods that have been previously described (Chen et al., 2011). The exchange vector for *Rosa26*$^{3TF.mCherry}$ was made by cloning both the mCherry DNA sequences and a 2A peptide-based expression cassette containing sequences for *Neurog3*, *Pdx1*, and *MafA* into separate sites of a pTRE-Tight-BI vector (Clontech). The bi-Tet operator assemblage was then inserted between the Lox71 and Lox2272 sites in pMCS.71/2272.Hygro. For the *Ptf1a*^{rtTA} allele, pPtf1a.Ex, a plasmid containing two inverted LoxP sites flanking the *Ptf1a* gene sequences and a FRT-flanked hygromycin-resistance cassette, was modified using standard methods to insert the 5' UTR sequences from *X. laevis*, rtTA sequences from pTET-ON Advanced vector (Clontech), and an intron-containing rabbit *beta-globin* poly A site. After electroporation of the exchange vectors into *Rosa26*^{LCA} (Chen et al., 2011) and *Ptf1a*^{LCA} containing mESCs (Burlison et al., 2008) respectively, clones surviving dual selection with hygromycin (Invitrogen) and gancyclovir (Sigma) were screened by PCR (**Table S6**). Blastocyst microinjections, chimeric matings and excision of the FRT-flanked hygromycin selection cassette were performed as previously described (Chen et al., 2011).

Immunoblot analysis. Pancreatic tissues were lysed in 20 mM Tris, pH 7.4, 20 mM NaCl, 1 mM EDTA, 20 mM beta-glycerophosphate, 5 mM EGTA, 1 mM PMSF, 1 µg/ml DTT, and 1x protease inhibitor (Sigma, P8340). Proteins were size fractionated in 4-20% SDS-PAGE gels (BioRad), transferred to polyvinylidene difluoride membranes (Millipore), blocked in 5% milk (BioRad) in PBS-T for 3 hours, then incubated with goat anti-Pdx1 (1:100; BCBC) or mouse anti-β actin (1:1000, Sigma) overnight at 4°C. The membranes were then washed, incubated with anti-goat and anti-mouse horseradish peroxidase-conjugated antibodies (Sigma) for 1 hour, washed again, then imaged using Western Lightning Plus ECL chemiluminescence kit (Perkin Elmer).

Luciferase Reporter Assays. The NeuroD1- and Insulin II-luciferase fusion gene constructs were previously described (Anderson et al., 2009; Zhao et al., 2005) as well as the design of the cytomegalovirus (CMV) enhancer-driven p300 (Lee et al., 1995), Beta2 (Qiu et al., 1998), and rtTA (Clontech 631069) expression vectors. Coding sequences for Neurog3, MafA, and Pdx1 were cloned into TRE-Tight (Clontech) in order to compare the function of the wild-type to the 2A peptide-modified variants. HeLa and Panc1 cell lines were grown in Dulbecco's modified Eagle's medium using 10% heat-inactivated fetal bovine serum, 25 mM glucose, penicillin (100 units/ml), and streptomycin (100 units/ml). To test the functionality of 2A peptide-modified MafA and Pdx1, HeLa cells were co-transfected in 6-well plates with CMV-driven rtTA (0.375 µg), p300 (0.375 µg), and Beta2 (0.375 µg) expression vectors and dox-inducible MafA (0.375 µg), Pdx1 (0.375 µg), or 3TF (0.375 µg) expression vectors in the presence of either -238 wild-type Insulin (0.375 µg), -238 Ins C1 mutant (0.375 µg), or -238 Ins A1/A3 mutant (0.375 µg) luciferase vectors. To test the functionality of 2A peptide modified Neurog3, Panc1 cells were co-transfected in 6-well plates with rtTA (0.5 µg) and either Ngn3 (0.5 µg) or 3TF (0.5 µg) in the presence of either the NDFull (0.5 µg) or NDΔ1 (0.5 µg) expression vectors. All transfections were performed using Polyfect Transfection reagent (Quiagen 301105) in the presence of dox (50 µM). A CMV-driven *Renilla* luciferase expression vector (7.5 ng) was used to correct for differences in transfection efficiency. Fusion gene expression was measured 40–48 hours after transfection using a Dual Luciferase reporter assay system (Promega) and an automated luminometer (BioTek). Each transfection condition was tested in triplicate (n=3). Firefly luciferase readings were normalized to *Renilla* luciferase values.

Antibodies for immunohistochemistry. All antibodies were used at a dilution of 1:1,000, except where otherwise noted: goat anti-Amylase (Santa Cruz Biotechnology, SC-212821), sheep anti-Somatostatin (ARP, 13-2366), rat anti-F4/80, 1:50 (Invitrogen MF48000), rat anti-CD45, 1:50 (BD Biosciences, 550539) rabbit anti-Chromogranin A (Abcam, ab15160), rabbit anti-Ghrelin (Phoenix Pharmaceuticals, G-031-30), rabbit anti-Glucagon (Linco, 4030-01F), guinea pig anti-Insulin (Invitrogen, 18-0067), rabbit anti-MafA, 1:500 (Bethyl laboratories, IHC-00352), goat anti-Neurog3 (BCBC, AB5684), guinea pig anti-Pdx1 (Gift of Chris Wright), guinea pig anti-Pancreatic polypeptide (Linco), rabbit anti-RFP (Rockland, 600-401-379), chicken anti-RFP (Rockland, 600-901-379), chicken anti-GFP (Invitrogen), and rabbit anti-Cytokeratin, 1:500 (Dako, Z0226). Secondary antibodies were from Invitrogen (donkey anti-rat Alexa Flour 488, goat anti-chicken Alexa Fluor 555, donkey anti-rabbit Alexa Flour 488 and Alexa Flour 555, donkey anti-goat Alexa Flour 488, donkey anti-sheep Alexa Flour 488, goat anti-guinea pig Alexa Flour 488), and Jackson ImmunoResearch (donkey anti-chicken Cy3).

FACS and RNA extraction. Pancreata were removed, perfused with 2.0 mg/mL collagenase P (Roche) in HBSS, minced and incubated at 37°C for 5 minutes. Cells were further dispersed by manual pipetting, washed with FACS staining buffer (R&D Systems), filtered through a 100 µm mesh cell strainer, then centrifuged. Cell pellets were resuspended in AccuMax (Sigma) and DNase1 (Ambion) and incubated at 37°C for 4 minutes. Afterwards,

cells were washed with FACS staining buffer, centrifuged, and resuspended in FACS buffer containing DNAse1 (1 U/ml, Ambion) and 1 mM EDTA. DAPI was used to stain for cell viability at a dilution of 1:1,000. Viable mCherry^{+} cells were sorted into TRIzol LS (Invitrogen) and total RNA was isolated using TRIzol LS (Invitrogen), DNase-treated, and column-purified (Zymo Research) as previously described (Osipovich et al., 2014).

RNA-seq pre-processing and differential expression analyses. Data were quantified and normalized with the PORT pipeline (https://github.com/itmat/Normalization; Kim *et al.*, manuscript in preparation). PORT extends the idea of resampling to resample for more than just read depth, but also for exon/intron/intergenic balance and ribosomal depletion balance (Li and Tibshirani, 2013). Moreover, PORT enables for separate treatment of genes that are predominantly expressed in a subset of the samples. This is particularly important in our case due to the peculiar composition of the acinar cell mRNA population. 90-95% of the mRNA molecules in a pancreatic acinar cell code for fewer than 30 secretory enzymes (Harding et al., 1977) and the Amylase-2a and Trypsinogen gene families have nearly identical members that account for nearly half of the mRNA molecules. We analyzed differential expression of non-protease genes with edgeR (FDR 0.01) (McCarthy et al., 2012) and PADE (FDR 0.1) (https://github.com/itmat/pade; this is an extension of PaGE,(Grant et al., 2005) in our 1 and 7 day induced acinar cells compared to uninduced acinar cells. Genes that were found to be differential expressed by both approaches were considered differential expressed.

Supplemental References

Anderson, K.R., Torres, C.A., Solomon, K., Becker, T.C., Newgard, C.B., Wright, C.V., Hagman, J., and Sussel, L. (2009). Cooperative transcriptional regulation of the essential pancreatic islet gene NeuroD1 (beta2) by Nkx2.2 and neurogenin 3. J Biol Chem *284*, 31236-31248.

Burlison, J.S., Long, Q., Fujitani, Y., Wright, C.V., and Magnuson, M.A. (2008). Pdx-1 and Ptf1a concurrently determine fate specification of pancreatic multipotent progenitor cells. Dev Biol *316*, 74-86.

Chen, S.X., Osipovich, A.B., Ustione, A., Potter, L.A., Hipkens, S., Gangula, R., Yuan, W., Piston, D.W., and Magnuson, M.A. (2011). Quantification of factors influencing fluorescent protein expression using RMCE to generate an allelic series in the ROSA26 locus in mice. Dis Model Mech *4*, 537-547.

Dore, B.A., Grogan, W.M., Madge, G.E., and Webb, S.R. (1981). Biphasic development of the postnatal mouse pancreas. Biol Neonate *40*, 209-217.

Grant, G.R., Liu, J., and Stoeckert, C.J., Jr. (2005). A practical false discovery rate approach to identifying patterns of differential expression in microarray data. Bioinformatics *21*, 2684-2690.

Harding, J.D., MacDonald, R.J., Przybyla, A.E., Chirgwin, J.M., Pictet, R.L., and Rutter, W.J. (1977). Changes in the frequency of specific transcripts during development of the pancreas. The Journal of biological chemistry *252*, 7391-7397.

Lee, J.S., Galvin, K.M., See, R.H., Eckner, R., Livingston, D., Moran, E., and Shi, Y. (1995). Relief of YY1 transcriptional repression by adenovirus E1A is mediated by E1A-associated protein p300. Genes & development *9*, 1188-1198.

Li, J., and Tibshirani, R. (2013). Finding consistent patterns: a nonparametric approach for identifying differential expression in RNA-Seq data. Statistical methods in medical research *22*, 519-536.

McCarthy, D.J., Chen, Y., and Smyth, G.K. (2012). Differential expression analysis of multifactor RNA-Seq experiments with respect to biological variation. Nucleic acids research *40*, 4288-4297.

Osipovich, A.B., Long, Q., Manduchi, E., Gangula, R., Hipkens, S.B., Schneider, J., Okubo, T., Stoeckert, C.J., Jr., Takada, S., and Magnuson, M.A. (2014). Insm1 promotes endocrine cell differentiation by modulating the expression of a network of genes that includes Neurog3 and Ripply3. Development *141*, 2939-2949.

Qiu, Y., Sharma, A., and Stein, R. (1998). p300 mediates transcriptional stimulation by the basic helix-loop-helix activators of the insulin gene. Mol Cell Biol *18*, 2957-2964.

Zhao, L., Guo, M., Matsuoka, T.A., Hagman, D.K., Parazzoli, S.D., Poitout, V., and Stein, R. (2005). The islet beta cell-enriched MafA activator is a key regulator of insulin gene transcription. J Biol Chem *280*, 11887-11894.